Spectral properties of ultracold Fermi gases

Eugen Dizer[1] Jan Horak[1] Jan M. Pawlowski[1,2]

[1]Institute for Theoretical Physics, Heidelberg University
[2]ExtreMe Matter Institute EMMI, GSI Darmstadt

STRUCTURES CLUSTER OF EXCELLENCE

UNIVERSITÄT HEIDELBERG ZUKUNFT SEIT 1386

ABSTRACT

The present work covers the following topics:

- Non-perturbative methods for strongly correlated ultracold Fermi gases
- Calculation of self-consistent spectral functions directly in real frequencies
- Comparison to recent experimental MIT data and other theoretical approaches
- Possible application to the superfluid phase of the BCS-BEC crossover

INTRODUCTION

Important properties of a Fermi gas, such as transport and scattering properties, or the excitation spectrum, are encoded in its spectral functions.

The computation of spectral functions requires access to the fermionic and bosonic self-energies at real frequencies [1, 2, 3]. However, standard numerical methods are formulated at imaginary frequencies [4].

The problem of analytic continuation

Analytic continuation of numerical data from $i\omega_n$ (Matsubara frequencies) to real frequencies ω poses an ill-conditioned task with large systematic uncertainties. In this work, we evaluate all quantities directly in real ω.

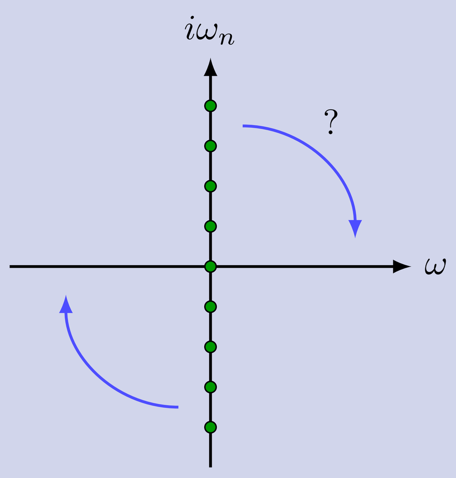

Figure 1. Wick rotation

BCS-BEC CROSSOVER

We consider a spin-balanced Fermi gas, where the contact interaction of fermions with opposite spin is modeled by the exchange of bosonic dimers,

$$S[\psi,\phi] = \int_0^\beta d\tau \int d^3x \Big[\sum_{\sigma=\uparrow,\downarrow} \psi_\sigma^*(\partial_\tau - \nabla^2 - \mu)\psi_\sigma + \nu\phi^*\phi - h\left(\phi^*\psi_\uparrow\psi_\downarrow - \phi\psi_\uparrow^*\psi_\downarrow^*\right) \Big] ,$$

where h is the Feshbach coupling between the fermions and bosons, and ν is the detuning of the dimer, which is connected to the scattering length a.

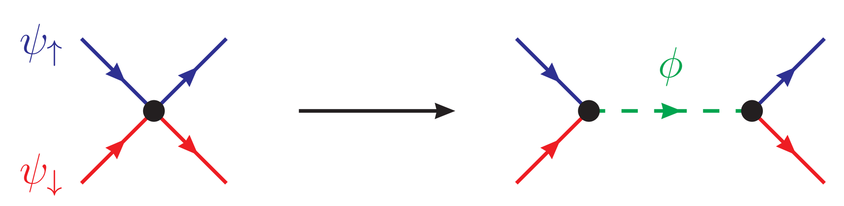

Figure 2. Hubbard-Stratonovich transformation.

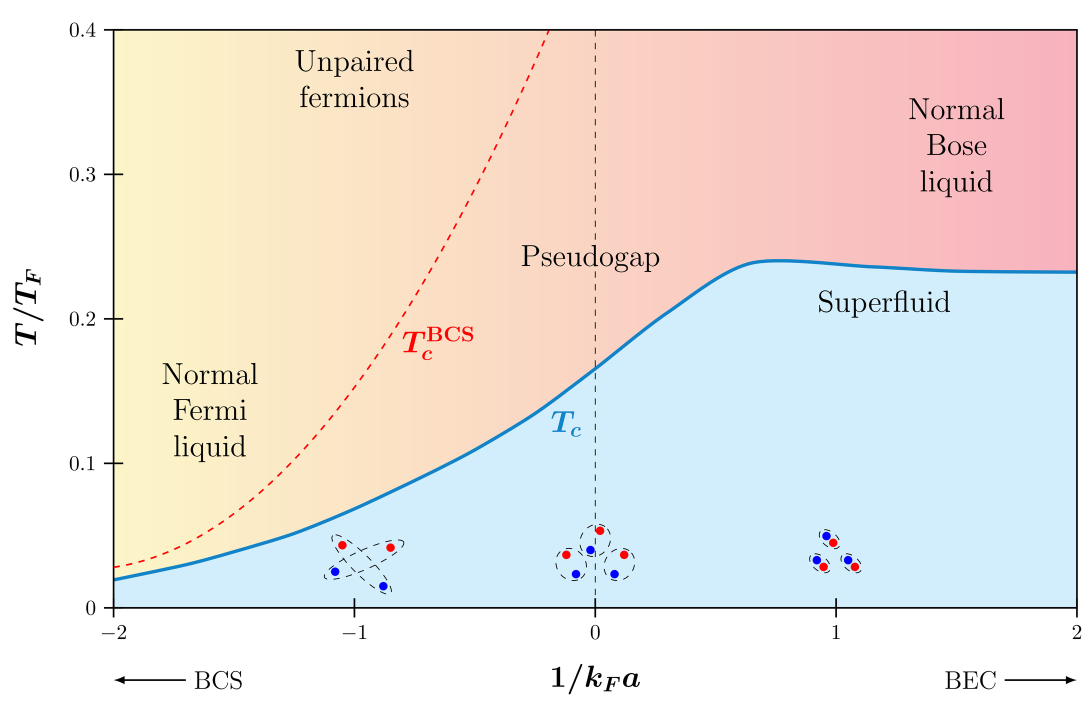

Figure 3. Phase diagram of the BCS-BEC crossover.

SPECTRAL FUNCTIONAL APPROACH

The self-consistent equations for the full propagators are derived using functional methods and read

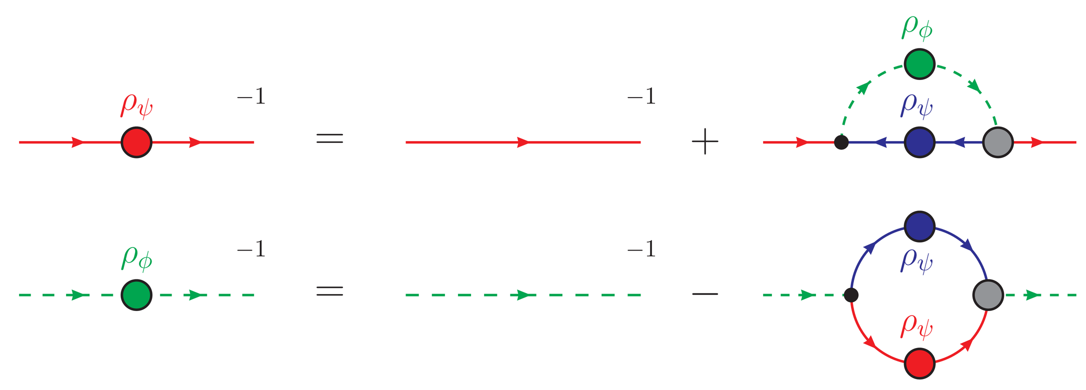

Figure 4. Self-consistent equations for the full spectral functions.

Spectral representation

We use the spectral representation of the propagators

$$G(i\omega_n, \boldsymbol{p}) = \int_{-\infty}^{\infty} d\lambda \, \frac{\rho(\lambda, \boldsymbol{p})}{-i\omega_n + \lambda} ,$$

where $\rho(\lambda, \boldsymbol{p})$ is the spectral function, which obeys

$$\rho(\omega, \boldsymbol{p}) = \frac{1}{\pi} \, \mathrm{Im}\, G^R(\omega, \boldsymbol{p}) ,$$

where ω is real and $G^R(\omega, \boldsymbol{p}) = G(\omega + i0^+, \boldsymbol{p})$ is the retarded propagator. In this way, we obtain direct equations for the spectral functions.

Evaluation at real frequencies

The limit $i\omega_n \to \omega + i0^+$ is performed analytically and yields for the imaginary part of the retarded self-energies

$$\boxed{\mathrm{Im}\, \Sigma_\psi^R(\omega, \boldsymbol{p})} \sim \int_{\lambda, \boldsymbol{q}} \boxed{\rho_\phi(\omega + \lambda, \boldsymbol{q})} \, \boxed{\rho_\psi(\lambda, \boldsymbol{q} - \boldsymbol{p})} \times \left[-n_B(\omega + \lambda) - n_F(\lambda) \right] ,$$

$$\boxed{\mathrm{Im}\, \Pi_\phi^R(\omega, \boldsymbol{q})} \sim \int_{\lambda, \boldsymbol{p}} \boxed{\rho_\psi(\omega - \lambda, \boldsymbol{p})} \, \boxed{\rho_\psi(\lambda, \boldsymbol{q} - \boldsymbol{p})} \times \left[1 - n_F(\omega - \lambda) - n_F(\lambda) \right] ,$$

with Fermi distribution n_F and Bose distribution n_B.

The real part is obtained from Kramers-Kronig relation

$$\mathrm{Re}\, \Sigma_\psi^R(\omega, \boldsymbol{p}) = \frac{1}{\pi} P \int_\lambda \frac{\mathrm{Im}\, \Sigma_\psi^R(\lambda, \boldsymbol{p})}{\lambda - \omega} .$$

RESULTS

Spectral functions

The spectral functions are calculated numerically by iteration directly in real frequencies.

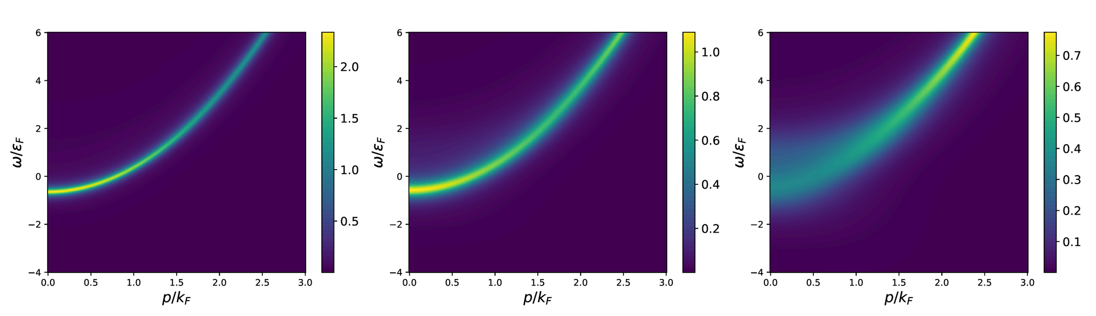

(a) $1/k_F a = -0.5$ (b) $1/k_F a = 0$ (c) $1/k_F a = 0.5$

Figure 5. Fermionic spectral function $\rho_\psi(\omega, \boldsymbol{p})\,\varepsilon_F$ for $T/T_F = 0.56$ at different interaction strengths $1/k_F a$.

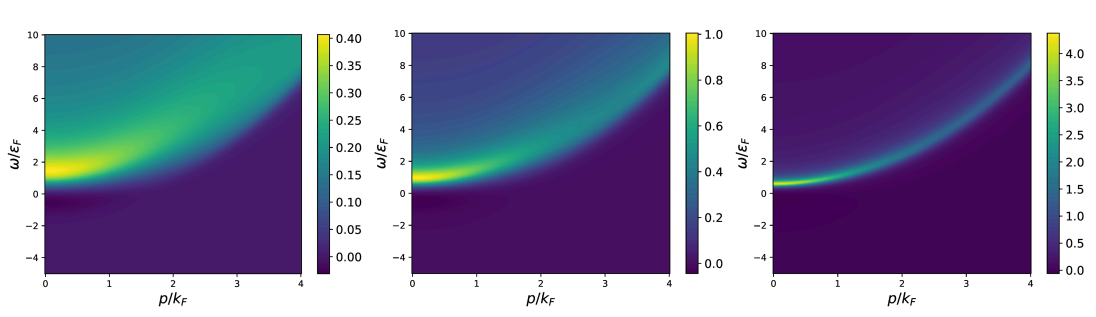

(a) $1/k_F a = -0.5$ (b) $1/k_F a = 0$ (c) $1/k_F a = 0.5$

Figure 6. Bosonic dimer spectral function $h^2 \rho_\phi(\omega, \boldsymbol{p})\,\sqrt{\varepsilon_F}/(8\pi)$ for $T/T_F = 0.56$ at different interaction strengths $1/k_F a$.

From the calculated spectral functions, we can obtain various observables of ultracold Fermi gases and compare with other approaches and the experiment.

Radio-frequency (Rf) spectra

The ejection rf spectrum $I(\omega)$ is calculated from the fermionic spectral function ρ_ψ by

$$I(\omega) = \int_{\boldsymbol{q}} \rho_\psi(\boldsymbol{q}^2 - \omega - \mu, \boldsymbol{q}) \, n_F(\boldsymbol{q}^2 - \omega - \mu) .$$

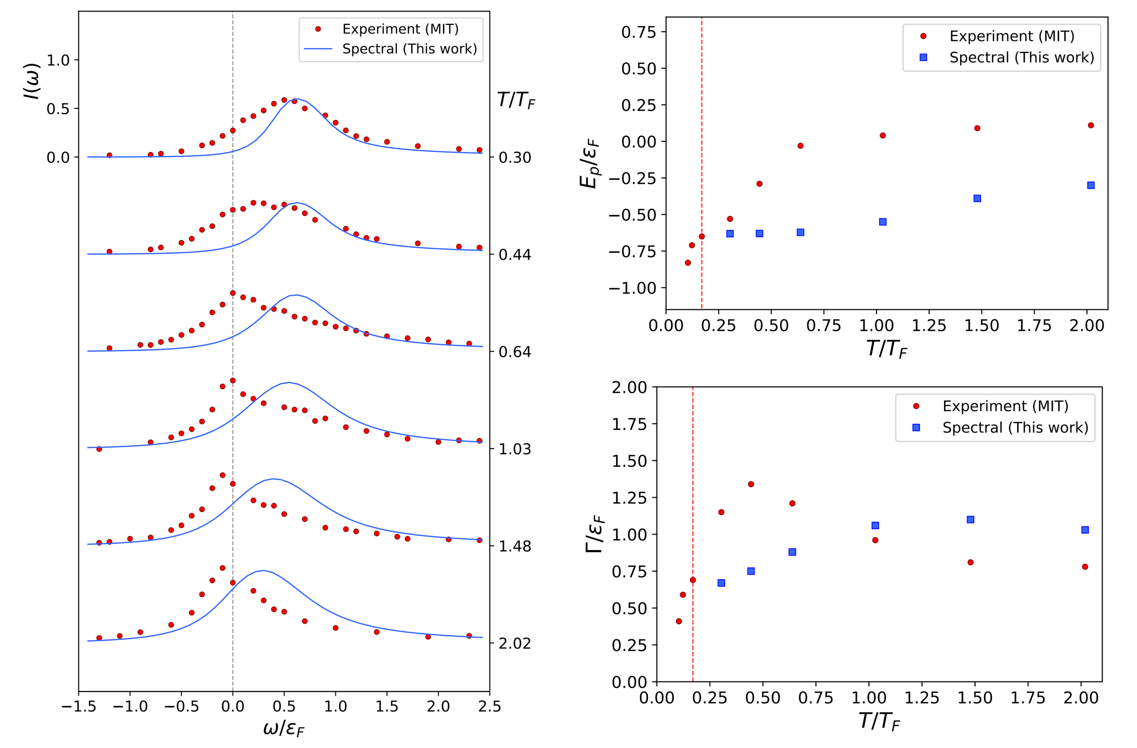

Figure 7. Rf spectra, peak positions ($E_p = -\omega_p$) and full width at half maximum Γ for the unitary Fermi gas in comparison to recent MIT data [5]. The red lines mark the superfluid phase transition.

Momentum distribution and density

The momentum distribution function $n(\boldsymbol{p})$ and total density n are calculated from the spectral function by

$$n(\boldsymbol{p}) = \int_\lambda \rho_\psi(\lambda, \boldsymbol{p}) \, n_F(\lambda) , \qquad n = 2 \int_{\boldsymbol{p}} n(\boldsymbol{p}) .$$

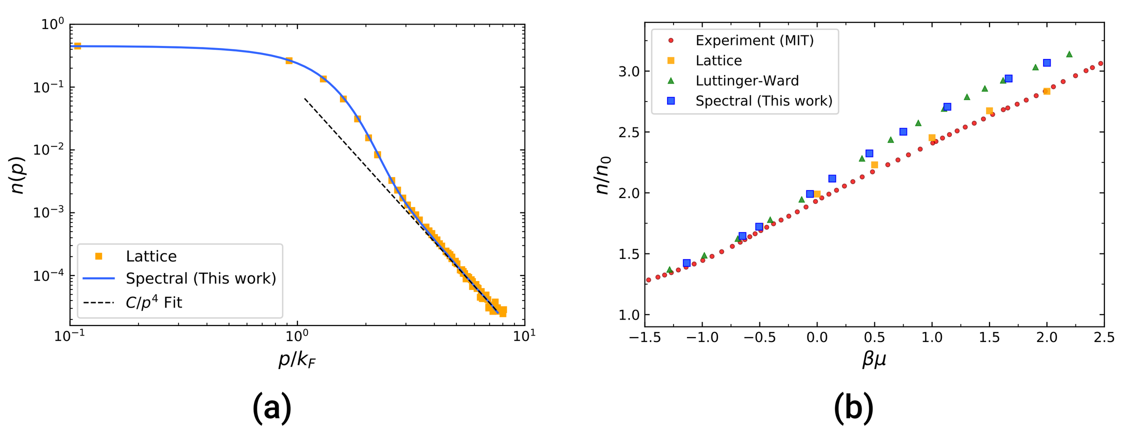

Figure 8. (a) Exemplary momentum density distribution $n(\boldsymbol{p})$ and (b) density equation of state for the unitary Fermi gas in comparison to other approaches and experiment.

SUMMARY AND CONCLUSIONS

We calculated self-consistent fermionic and bosonic spectral functions in the normal phase of a 3D Fermi gas directly in real-time.

The present approach opens the path towards:

- Transport properties and calculation of spectral functions in the superfluid phase of ultracold Fermi gases
- Inclusion of vertex corrections and other classes of diagrams towards full quantitative precision

REFERENCES

[1] Eugen Dizer, Jan Horak, and Jan M. Pawlowski. *arXiv:2311.16788*, Nov 2023.

[2] Tilman Enss. *arXiv:2311.05443*, Nov 2023.

[3] Christian H. Johansen, Bernhard Frank, and Johannes Lang. *arXiv:2311.03953*, Nov 2023.

[4] Rudolf Haussmann, Matthias Punk, and Wilhelm Zwerger. *Phys. Rev. A*, 80:063612, Dec 2009.

[5] Biswaroop Mukherjee, Parth B. Patel, Zhenjie Yan, Richard J. Fletcher, Julian Struck, and Martin W. Zwierlein. *Phys. Rev. Lett.*, 122:203402, May 2019.